

# JET ENTRAINMENT AND COMPRESSION IN COMPRESSIBLE FLOW EJECTORS

S.K. CHOU

DEPARTMENT OF MECHANICAL & PRODUCTION ENGINEERING  
NATIONAL UNIVERSITY OF SINGAPORE, KENT RIDGE, SINGAPORE 0511

**SUMMARY** Entrainment and compression of a secondary subsonic fluid stream by a primary jet in the mixing chamber of an ejector is investigated. A one-dimensional approach is adopted and the resultant matrix equation is solved for the static-pressure rise in a variable-area mixing chamber. The analysis, based on average properties of the two streams, incorporates an interface force between the streams expressed as a function of the dimensions of the mixing zones. Different empirical factors of the interface force are applied along the axial flow-field and comparisons are made between analytical and experimental results. A discussion on the influence of these empirical factors on the behaviour of the flow in terms of velocity and pressure variations is also presented.

## 1. NOTATION

A	= area
C	= average fluid velocity
$C_{01}$	= fluid velocity of primary stream at nozzle exit
$A_m$	= mass amplification, $A_m = (m_1 + m_2)/m_1$
D	= mixing chamber diameter
L	= length of mixing chamber excluding diffuser
$C_p$	= specific heat at constant pressure
$F_1$	= interface force per unit area
$F_2$	= wall friction force per unit area
h	= specific enthalpy
m	= mass flow
Q	= heat transfer
W	= work transfer
p, P	= absolute pressure
T	= absolute temperature
k	= heat transfer fraction
$f_1$	= interface force factor
$f_2$	= wall friction factor
$f_{e1}, f_{e2}, f_{e3}, f_{x1}$	= empirical factors in mixing zones
$\Delta x$	= increment of axial distance, x
$x_1, x_2, x_3$	= zone positions
$\Delta p$	= pressure parameter, $\Delta p = (p - p_0)/(p_{01} - p_0)$
$\rho$	= average fluid density
$\alpha$	= cone angle of mixing chamber
$\phi$	= primary stream angle of spread

## SUBSCRIPTS

0	= stagnation conditions
1	= primary stream
2	= secondary stream
d	= exit of ejector
t	= primary nozzle throat

## 2. INTRODUCTION

An ejector is a device comprising of a system of nozzles, commonly arranged axisymmetrically, for the purpose of allowing a motive fluid to entrain and compress a secondary fluid stream. Applications of the device may be found in fluid mixing, flame stabilization, boundary-layer control, refrigeration exhaust and ventilation. Analyses related to jet entrainment and compression in ejectors have been sufficiently detailed and notable studies include: compound flow behaviours within nozzles by Bernstein et al (1967), the use of a constant turbulent Reynolds number in incompressible jet mixing by Hill (1967), an integral method employing a polynomial

velocity profile and the testing of a high mass ratio air-air ejector by Hickman et al (1972), a finite-difference two-dimensional flow model by Hedges and Hill (1974), the phenomena of choking and mixing by Otis (1976) and flow-field measurements by Helmbold et al (1954). The present study is an attempt at understanding the mechanisms of entrainment and compression in compressible flow ejectors having variable-area mixing chambers of known dimensions. The numerical solution proceeds, by using step-wise increments of the mixing chamber length, towards velocity equilibration between the two streams, thereby, obtaining the pressure distribution along the flow. Tests on an air-air ejector provide experimental data for the determination of empirical factors used in the numerical computations.

## 3. ANALYSIS

A one-dimensional flow model is formulated as an extension to the one developed by Otis (1976). Referring to Fig. 1, the complex mixing mechanism between the two streams has been greatly simplified by the introduction of an interface force between them. The more energetic primary flow is seen to decelerate while entraining the slower secondary stream against the wall friction and possible adverse pressure gradients. Assumptions made on the flow include: adiabatic mixing, identical and perfect gases, no condensation shocks, absence of recirculating flows and pressure equilibration between streams at every section of the mixing chamber.

From Fig. 1, the following equations for the two streams may be written:

### Energy Equation:

$$\Delta Q_1 - \Delta W_1 = m_1 \Delta h_1 + m_1 C_{p1} \Delta C_1 \quad (1)$$

$$\text{and } \Delta Q_2 - \Delta W_2 = m_2 \Delta h_2 + m_2 C_{p2} \Delta C_2 \quad (2)$$

### Momentum Equation:

For the primary stream:

$$-F_1 \Delta A_1 \cot \phi - (p + \Delta p)(A_1 + \Delta A_1) + (p + \Delta p/2) \Delta A_1 + p A_1 = m_1 \Delta C_1 \quad (3)$$

and for the secondary stream:

$$F_1 \Delta A_1 \cot \phi - F_2 \Delta A_2 \cot \alpha - (p + \Delta p)(A_2 + \Delta A_2) + (p + \Delta p/2) \Delta A_2 + p A_2 = m_2 \Delta C_2 \quad (4)$$

where  $\Delta A = \Delta A_1 + \Delta A_2$

Neglecting higher order terms, equations (3) and (4) may be rewritten as

$$-F_1 \Delta A_1 \cot \phi - A_1 \Delta p = m_1 \Delta C_1 \quad (5)$$

$$F_1 \Delta A_1 \cot \phi - F_2 \Delta A \cot \alpha - A_2 \Delta p = m_2 \Delta C_2 \quad (6)$$

where  $\Delta A_1 \cot \phi = \pi d_1 \Delta x$

and  $\Delta A \cot \alpha = \pi D \Delta x$

Mass Conservation Equation:

$$\Delta \rho_1 / \rho_1 + \Delta C_1 / C_1 + \Delta A_1 / A_1 = 0 \quad (7)$$

$$\text{and } \Delta \rho_2 / \rho_2 + \Delta C_2 / C_2 + \Delta A_2 / A_2 = 0 \quad (8)$$

where  $\Delta A_2 = \Delta A - \Delta A_1$

Equation of State:

$$\Delta \rho_1 / \rho_1 + \Delta T_1 / T_1 - \Delta p / p = 0 \quad (9)$$

$$\text{and } \Delta \rho_2 / \rho_2 + \Delta T_2 / T_2 - \Delta p / p = 0 \quad (10)$$

with the assumption that pressure equilibration occurs at every section along the mixing zone.

The work and heat transfer terms in equations (1) and (2) may be taken as arising from the presence of the interface force,  $F_1$ . Thus, the work done by stream 1 is

$$\Delta W_1 = C_1 F_1 \pi d_1 \Delta x \quad (11)$$

and the work done on stream 2 is

$$\Delta W_2 = -C_2 F_1 \pi d_1 \Delta x \quad (12)$$

Since  $\Delta W_1$  and  $\Delta W_2$  are not equal, the difference may be regarded as heat generated and the fractions deposited in both streams are:

$$\Delta Q_1 = k(C_1 - C_2) F_1 \pi d_1 \Delta x \quad (13)$$

$$\text{and } \Delta Q_2 = (1-k)(C_1 - C_2) F_1 \pi d_1 \Delta x \quad (14)$$

Upon substituting for the enthalpy, work and heat transfer terms in equations (1) and (2), the energy equations are rewritten as

$$m_1 C_p \Delta T_1 + m_1 C_1 \Delta C_1 = [k(C_1 - C_2) - C_2] F_1 \pi d_1 \Delta x \quad (15)$$

$$\text{and } m_2 C_p \Delta T_2 + m_2 C_2 \Delta C_2 = [(1-k)(C_1 - C_2) + C_2] F_1 \pi d_1 \Delta x \quad (16)$$

Equations (5) to (10), (15) and (16) may be expressed in matrix form with non-dimensional variables as,

$$\begin{bmatrix} C_1^2 & \frac{C_{pn} C_1}{P_{mo}} & 0 & 0 & 0 & 0 & 0 & 0 & 0 \\ 0 & 0 & 0 & C_2^2 & \frac{C_{pn} C_2}{P_{mo}} & 0 & 0 & 0 & 0 \\ C_1 & 0 & 0 & 0 & 0 & 0 & \frac{1}{\rho_1 X_{mo}} & 0 & 0 \\ 0 & 0 & 0 & C_2 & 0 & 0 & \frac{1}{\rho_2 X_{mo}} & 0 & 0 \\ 0 & \frac{1}{T_1} & \frac{1}{\rho_1} & 0 & 0 & 0 & -\frac{1}{P} & 0 & 0 \\ 0 & 0 & 0 & 0 & \frac{1}{T_2} & \frac{1}{\rho_2} & -\frac{1}{P} & 0 & 0 \\ \frac{1}{C_1} & 0 & \frac{1}{\rho_1} & 0 & 0 & 0 & 0 & 0 & \frac{1}{A_1} \\ 0 & 0 & 0 & \frac{1}{C_2} & 0 & \frac{1}{\rho_2} & 0 & 0 & -\frac{1}{A_2} \end{bmatrix} \begin{bmatrix} \Delta C_1 \\ \Delta T_1 \\ \Delta \rho_1 \\ \Delta C_2 \\ \Delta T_2 \\ \Delta \rho_2 \\ \Delta P \\ \Delta A_1 \end{bmatrix} = \begin{bmatrix} [(k-1)C_1 - kC_2] (2f_1) \left(\frac{L_m}{d}\right) \left(\frac{\rho_1}{\rho_2}\right) (C_1 - C_2)^2 \\ [C_1 - k(C_1 - C_2)] (2f_1) \left(\frac{L_m}{d}\right) \left(\frac{1}{\rho_2}\right) \delta_1 (C_1 - C_2)^2 \\ -2f_1 \left(\frac{L_m}{d}\right) (C_1 - C_2)^2 \\ 2f_1 \left(\frac{L_m}{d}\right) \left(\frac{\rho_1}{\rho_2}\right) \delta_1 (C_1 - C_2)^2 - 2f_2 \frac{L_m}{D} \delta_2 C_2^2 \\ 0 \\ 0 \\ 0 \\ -\Delta A / A_2 \end{bmatrix} \quad (17)$$

with dimensionless terms expressed as:

$$C_1 = C_1 / C_{o1} \quad C_2 = C_2 / C_{o1} \quad T_1 = T_1 / T_{o1} \quad T_2 = T_2 / T_{o1}$$

$$\rho_1 = \rho_1 / \rho_{o1} \quad \rho_2 = \rho_2 / \rho_{o1} \quad P = P / P_{o2} \quad A_1 = A_1 / A_t$$

$$A_2 = A_2 / A_t \quad C_{pn} = 1 \quad P_{mo} = C_{o1}^2 / C_p T_{o1} \quad X_{mo} = \rho_{o1} C_{o1}^2 / P_{o2}$$

$$L_m = \Delta x / d_t \quad \delta_1 = d_1^2 / (D^2 - d_1^2) \quad \delta_2 = D^2 / (D^2 - d_1^2)$$

$$D_m = D / dt \quad d = d_1 / dt \quad \text{and}$$

$$\text{Interface force, } F_1 = f_1 \rho_1 (C_1 - C_2)^2 / 2$$

$$\text{Friction force, } F_2 = f_2 \rho_2 C_2^2 / 2$$

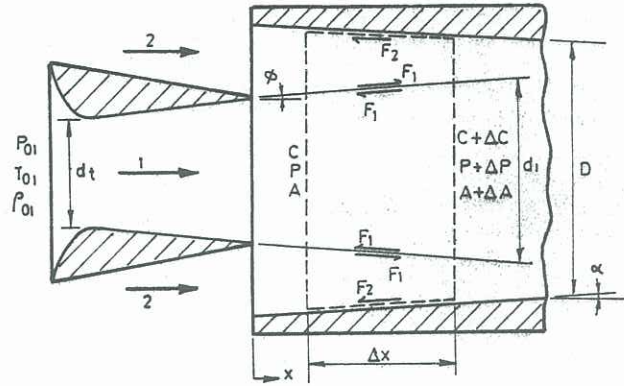


Fig. 1 Elemental volume of mixing zone

#### 4. EXPERIMENT

The experimental ejector system consists of a primary convergent-divergent nozzle and a mixing chamber within an ejector housing. Both the nozzle and chamber are made of bronze and arranged axisymmetrically as shown in Fig. 2. The mixing chamber's convergent and diffuser sections have total cone angles of 3 and 8 degrees, respectively. The test set-up is shown schematically in Fig. 3. Air at a specified pressure was supplied to the primary nozzle by way of an air-box downstream of the primary control valve. Further upstream, compressed air from the receiver was first dried through a moisture separator before regulation. The secondary air supply condition was controlled by a secondary valve. At the exit of the ejector, the discharge pressure was regulated by a back-pressure control valve.

Measurements of mass flow were made using rotameters and calibrated orifice plates. Bourdon gauges were employed for static pressure measurements while well-embedded thermocouples were used for temperature measurements. Pressure variations along the mixing chamber were recorded by a multi-tube mercury manometer from pressure tapings spaced at 15mm intervals.

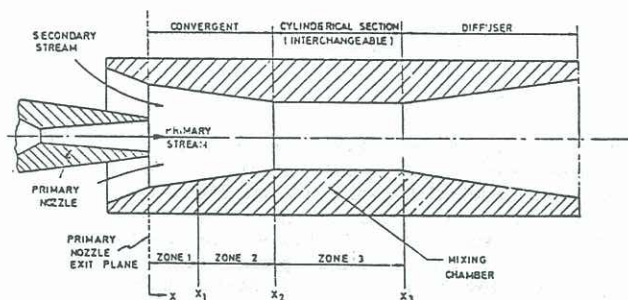


Fig. 2 Nozzle arrangement and mixing zones

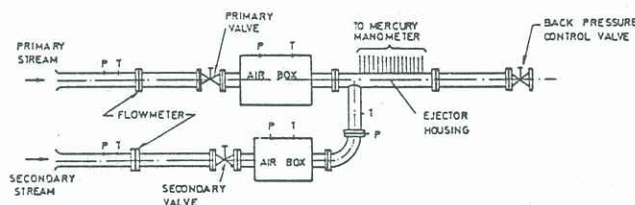


Fig. 3 Layout of ejector test rig

## 5. NUMERICAL COMPUTATION

Equation (17) is numerically solved by employing step-wise increments,  $\Delta x$ , of the mixing chamber length. The new values of all variables at the  $(n+1)^{th}$  step are evaluated by adding the increments calculated to the values at the  $n^{th}$  step. The numerical integration begins at the primary nozzle exit plane and ends at the entrance to the diffuser.

Three zones within the mixing chamber are defined as shown in Fig. 2. From experimental data, the zones were chosen to reflect changes in the pressure distribution along the axial flow-field. The interface force factor,  $f_1$ , used in each zone, is given as:

$$\text{Zone 1: } f_1 = f_{e1} (d_1/D) \text{ for } 0 < x < x_1$$

$$\text{Zone 2: } f_1 = f_{x1} + f_{e2} (x-x_1)/(x_2-x_1)$$

$$\text{where } x_1 < x < x_2 \text{ and } f_{x1} = f_1 \text{ at } x = x_1$$

$$\text{Zone 3: } f_1 = f_{e3} \text{ for } x_2 < x < x_3$$

Throughout this study, it has been assumed that the heat generated between the streams was equally deposited in the streams. Hence, the value of  $k$ , the heat transfer fraction, was taken as 0.5.

## 6. DISCUSSION

In zone 1, up to 8 nozzle-throat diameters from the exit plane, the wall-pressure remains practically constant as may be seen in Figs. 4 to 6 where experimental data up to the entrance to the diffuser are shown. Here, the secondary fluid is sucked into the annulus region around the primary jet and the difference in velocity between the two streams is great. The interface force hardly comes into play and the rate of spreading of the primary jet is relatively low. The value of the empirical constant,  $f_{e1}$ , lies between 0.024 and 0.045, increasing with increasing length-to-diameter ratio of zone 1. It has been found that the value of  $f_{e1}$  has minimal effect on both the pressure profile and the velocity distribution of the flow. Factors which influence the length of zone 1 include the mass amplification and the back pressure of the ejector.

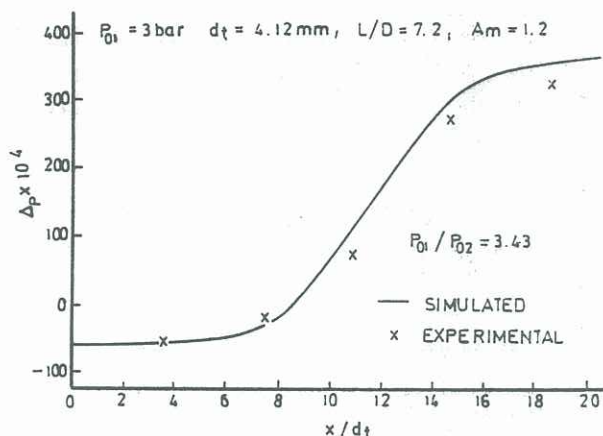


Fig. 4 Pressure variation in mixing chamber

The flow in zone 2 is characterised by an abrupt pressure rise which terminates at the entrance to the cylindrical section of the mixing chamber. Here, the interface force factor,  $f_1$ , increases steadily and linearly with distance. The primary fluid stream decelerates as entrainment of the secondary stream intensifies, and the difference in velocity of the two streams reduces. In this zone, the empirical constant,  $f_{e2}$ , has a strong influence on the flow behaviour. Its value is found to be between 0.15 and 0.30 - the higher the value, the more rapid are the pressure rise and convergence of fluid velocities.

In zone 3, the final stage of entrainment before diffusion, pressure variations are observed to be gradual. In shorter chambers, the fluid pressure continues to rise and this trend is observed for a chamber length-to-diameter ratio of up to about 14. For longer chambers, pressure losses are observed and compression efficiency falls with increasing chamber length. The interface force factor is taken as constant, characterising the fully developed nature of the flow, and the value of  $f_{e3}$  is found between 0.02 and 0.04. The influence of  $f_{e3}$  on the pressure profile and fluid velocities is generally weak. At entry to the diffuser, the secondary stream velocity is within 70 to 80 percent of the primary stream.

The simulated pressure distributions are given in Figs 4 to 6. In solving equation (17) a check for singularities in the flow was made at each step by

employing the compound-flow indicator,  $\beta$  developed by Bernstein et al (1967), namely,

$$\beta = \frac{n}{\sum_{i=1}^n A_i (1-M_i^2) / k_i M_i^2}$$

where  $A_i$ ,  $M_i$  and  $k_i$  are the flow area, the Mach number and the ratio of specific heats of the  $i^{\text{th}}$  stream, respectively. In this study,  $\beta$  was calculated at each increment,  $\Delta x_i$ . It was found that the value of  $\beta$  was always positive, implying that the flows studied were compound-subsonic.

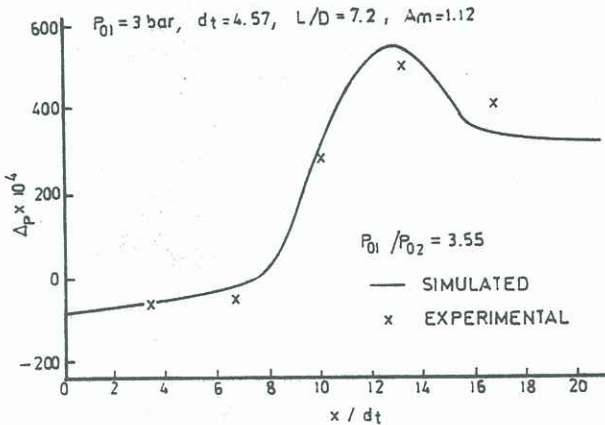


Fig. 5 Pressure variation in mixing chamber

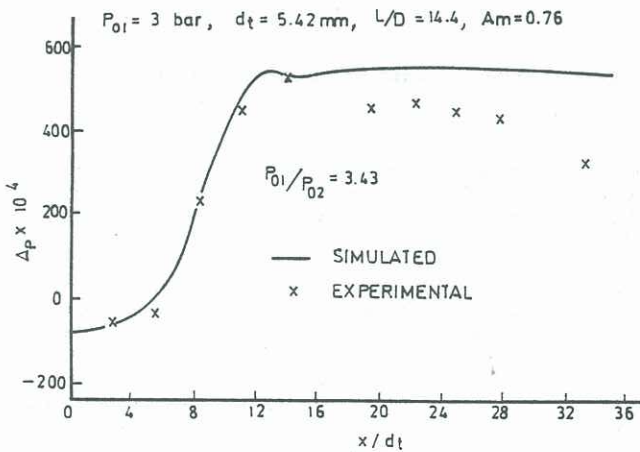


Fig. 6 Pressure variation in mixing chamber

## 7. CONCLUSION

The flow behaviour within compressible flow ejectors was studied. A one-dimensional flow model was used and jet entrainment and compression mechanisms were characterised by an interface force between the streams expressed in terms of empirical constants and mixing chamber dimensions. The mixing chamber was zoned according to distinct pressure profiles obtained from experiments. Tests were carried out on an air-air jet pump having primary nozzle-to-mixing chamber diameter ratios between 0.29 to 0.39. Simulated results were compared with experimental

data and the empirical constant for each zone obtained. Further work on multi-stream flow and investigations on the significance of the interface forces will be necessary for a better understanding of the complexities of jet entrainment and compression in compressible flow ejectors.

## 8. ACKNOWLEDGEMENTS

The author wishes to thank Mr. Y P Chua and Mr. P L Eu for their collaboration in this study, and the National University of Singapore for financial support under a research grant, RP28/82.

## 9. REFERENCES

- BERNSTEIN, A., HEISER, W.H. and HEVENOR, C. (1967) Compound-Compressible Nozzle Flow. *J. of Applied Mechanics*, TRANS ASME, Vol. 34, pp. 548-554.
- HEDGES, K.R. and HILL, P.G. (1974) Compressible Flow Ejectors, Part 1 - Development of a Finite-Difference Flow Model. *J. of Fluids Engineering*, TRANS ASME, Vol. 96, pp. 272-281.
- HELMBOLD, H.B., LUESSEN, G. and HEINRICH, A.M. (1954) An Experimental Comparison of Constant Pressure and Constant Diameter Jet Pumps. University of Wichita, School of Engineering, Engineering Report No. 147.
- HICKMAN, K.E., HILL, P.G. and GILBERT, G.B. (1972) Analysis and Testing of Compressible Flow Ejectors with Variable Area Mixing Tubes. *J. of Basic Engineering*, TRANS ASME, Vol. 94, pp. 407-416.
- HILL, P.G. (1967) Incompressible Jet Mixing in Converging-Diverging Axisymmetric Ducts. *J. of Basic Engineering*, TRANS ASME, Vol. 89, pp. 210-220.
- OTIS, D.R. (1976) Choking and Mixing of Two Compressible Fluid Streams. *J. of Fluids Engineering*, TRANS ASME, Vol. 98, pp. 311-317.